International Conference on Control, Automation and Systems 2010
Oct. 27-30, 2010 in KINTEX, Gyeonggi-do, Korea

Wide-Angle Laser Structured Light System Calibration with a Planar Object

Daesik Kim[1], Seongsoo Lee[1], Hyunwoo Kim[2] and Sukhan Lee[1]

[1] Department of Electrical and Computer Engineering, Sungkyunkwan University, Suwon, Korea
(Tel : +82-31-299-6477; E-mail: {daesik80, lsh}@ece.skku.ac.kr)
[2] Department of Computer Science and Engineering, Hanyang University, Ansan, Korea

Abstract: In this paper, we proposed a calibration method for a structured light system composed of a wide-angle line laser and a camera using a planar object. Instead of directly calibrating the camera with a planar object, we separated the radial distortion estimation from the camera calibration step to improve accuracy. Firstly, we corrected the lens radial distortion and then computed the camera's intrinsic and extrinsic parameters. For line laser calibration, the line laser's position was extracted from the distorted image. The laser's sub-pixel position was then calculated using the proposed normalized weighted average method, and forward-mapped to the rectified image. The corresponding 3D point of the extracted laser was estimated by computing the intersecting point of the camera ray and the calibration plane. The experimental results show the superiority of the proposed method.

Keywords: laser structured light system, calibration, wide-angle lens, sub-pixel, normalized weighted average

1. INTRODUCTION

A line laser-based structured light system has been used for several decades in many research fields because of its highly accurate 3D measurement ability. Recently, wide-angle cameras have become very popular for several applications, such as robotics and surveillance, which has caused an increased demand for wide-angle 3D measurement. In order to obtain good 3D results with a wide-angle structured light system, calibration should be carefully performed especially considering the fact that a wide-angle camera has severe lens distortion.

In this paper, we proposed a calibration method for a structured light system utilizing a wide-angle laser and a camera. First, we calibrated the camera and then computed the laser's (light) plane equation. This paper's contributions are: (1) we have demonstrated a calibration method using a planar object instead of a 3D object; (2) we have compensated the radial distortion to improve the accuracy of the camera calibration result; (3) we have extracted the 2D laser point in sub-pixel with the proposed *normalized weighted average*; and (4) we have detected all points in the distorted image plane and forward-mapped to the rectified image plane for a more accurate detection.

This paper's organization is as follows. Section 2 describes the calibration method of the proposed structured light system and the sub-pixeling methods are introduced in section 3. The experimental results are illustrated in section 4.

2. LASER STRUCTURED LIGHT SYSTEM CALIBRATION

The calibration of the laser structured light system can be divided into camera calibration and line laser calibration. The camera calibration is used to compensate the radial distortion and estimate intrinsic and extrinsic parameters. The line laser calibration is used to obtain the (light) plane equation with respect to the camera coordinate frame.

2.1 Camera Calibration

Instead of directly calibrating the camera with a chessboard planar object, we separated the radial distortion estimation from the camera calibration step to improve accuracy. We first corrected the lens radial distortion and then computed the camera's intrinsic and extrinsic parameters (transformation between the camera and the calibration plane).

For correction of lens radial distortion, we applied the FOV model proposed by [1]. This model has a single parameter, which is the field of view ω, and the distortion function and its inverse are

$$r_d = \frac{1}{\omega}\arctan\left(2r_u \tan\frac{\omega}{2}\right), \qquad r_u = \frac{\tan(r_d\omega)}{2r_u \tan\frac{\omega}{2}}, \tag{1}$$

where $r_d = \sqrt{x_d^2 + y_d^2}$, $r_u = \sqrt{x_u^2 + y_u^2}$, (x_d, y_d) is the distorted image point, and (x_u, y_u) is the undistorted image point. The advantage of the distortion model in [1] is that the forward and its inverse model are clearly given, so the approximation of the inverse model required in most other methods (because of the nonlinear transformation) is not required.

The other camera parameters except the distortion coefficients, such as focal length and principal point, can then be estimated using Zhang's planar object-based calibration method [2]. As the image becomes unclear and blurred when the distorted image is rectified, the accuracy of the corner position decreases during corner extraction in the rectified (i.e., undistorted) image plane. Therefore, we extracted the corners (x_d, y_d) of the chessboard calibration plane in the *i*-th distorted image, and it is forward-mapped into the rectified image. These forward-mapped points (x_d, y_d) are then used in camera calibration. We used the OpenCV for computing the camera parameters.

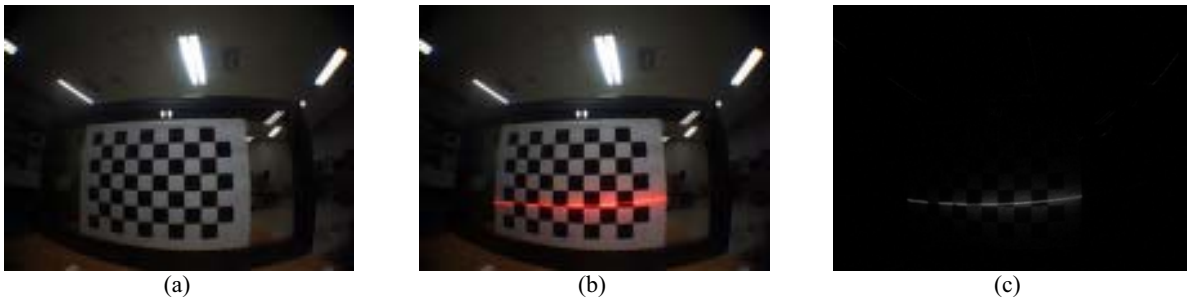

(a) (b) (c)

Figure 1. (a) chessboard image, (b) laser-added image, (c) laser-only image

2.2 Line Laser Calibration

In this paper, we regard the line laser as a light plane, so the procedure of the line laser calibration involved the estimation of the (light) plane equation with respect to the camera frame.

After grabbing the chessboard image I^i (figure 1 (a)), we additionally projected the line laser to the calibration plane and obtained the laser-added image J^i (figure 1 (b)). Here, the superscript *i* indicates the *i*-th chessboard image. The location of the calibration plane in I^i and J^i should be fixed in space. We subtracted I^i from J^i so as to obtain the laser-only image K^i (figure 1 (c)):

$$K^i = J^i - I^i \tag{2}$$

We extracted the laser's position in K^i and found the sub-pixel position by calculating the normalized weighted average we had proposed in section 3.3. This approach showed a more accurate line localization compared with that of the ordinary sub-pixeling method. The laser's 2D coordinates were then forward-mapped to the rectified image plane.

The next step is verifying if the laser is inside of the calibration plane. Let $\mathbf{p}_0$ be the laser point, $\mathbf{p}_m$ be the one of the outer corner points of the chessboard plane and $\mathbf{v}_m = \mathbf{p}_m - \mathbf{p}_0$ (m=1, 2, 3, 4) be the vector between these points (see figure 2). By the definition of the inner product, the angle θ_m between the successive vectors is

$$\theta_m = \cos^{-1} \frac{\mathbf{v}_m \cdot \mathbf{v}_n}{|\mathbf{v}_m||\mathbf{v}_n|}, \tag{3}$$

where

$$\begin{cases} n = m+1 & \text{if } (m < 4) \\ n = 1 & \text{otherwise} \end{cases}.$$

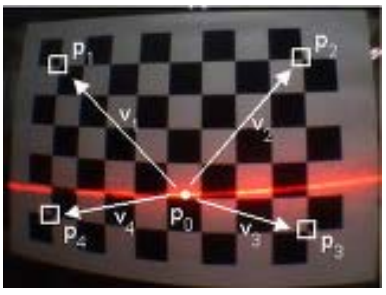

Figure 2. How to verify $\mathbf{p}_0$ if it is inside the chessboard.

If the laser point, $\mathbf{p}_0$ is inside the square generated by four outer corner points $\mathbf{p}_m$, the sum of these angles in (3) becomes $360°$:

$$\sum_{m=1}^{4} \theta_m = 360° . \tag{4}$$

We repeat this process for all chessboard images.

As line laser calibration involves the estimation of the light plane equation with respect to the camera frame, we first estimate the 3D point corresponding to the extracted 2D laser. Such can be performed by computing the intersecting point of the camera ray and the calibration plane. As we know the transformation (i.e., extrinsic parameters) between the camera and the calibration plane, the plane can be transformed and represented with respect to the camera coordinate frame.

When the coordinate frame is aligned with the *i*-th calibration plane frame, the normal vector of the plane is

$$\mathbf{n}^i = [0 \;\; 0 \;\; 1]^\mathsf{T}, \tag{5}$$

and the origin of the plane is

$$\mathbf{o}^i = [t_x^i \;\; t_y^i \;\; t_z^i]^\mathsf{T}, \tag{6}$$

where t_x^i, t_y^i, t_z^i are the translations in *x*, *y*, and *z* axis between the camera and the *i*-th plane, respectively. We can rotate this plane with respect to the camera coordinate frame because we already know the rotations:

$$\mathbf{n}^{i\prime} = \mathbf{R}^i \cdot \mathbf{n}^i = \begin{bmatrix} r_{11}^i & r_{12}^i & r_{13}^i \\ r_{21}^i & r_{22}^i & r_{23}^i \\ r_{31}^i & r_{32}^i & r_{33}^i \end{bmatrix} \begin{bmatrix} 0 \\ 0 \\ 1 \end{bmatrix} = \begin{bmatrix} r_{13}^i \\ r_{23}^i \\ r_{33}^i \end{bmatrix} = \begin{bmatrix} a^i \\ b^i \\ c^i \end{bmatrix}, \tag{7}$$

where $\mathbf{R}^i$ is the *i*-th rotation matrix and $\mathbf{n}^{i\prime}$ is the normal vector represented with respect to the camera coordinate frame, whose plane equation is

$$a^i X + b^i Y + c^i Z + d^i = 0 . \tag{8}$$

By plugging the origin of the *i*-th plane $\mathbf{o}^i$ into (8), the distance d^i can be computed:

$$d^i = -(a^i t_x^i + b^i t_y^i + c^i t_z^i) . \tag{9}$$

Now, we obtained the *i*-th plane equation with respect to the camera coordinate frame. The remaining problem is the estimation of the 3D point $\tilde{\mathbf{X}}_j^i = [X_j^i \;\; Y_j^i \;\; Z_j^i]^\mathsf{T}$ corresponding to the *j*-th 2D laser point $\mathbf{x}_j^i = [x_j^i \;\; y_j^i \;\; 1]^\mathsf{T}$ in *i*-th image. The relationship between $\tilde{\mathbf{X}}_j^i$ and $\mathbf{x}_j^i$ is as follows:

$$s\mathbf{x}_j^i = \mathbf{K}\tilde{\mathbf{X}}_j^i, \tag{10}$$

where **K** is the intrinsic parameter matrix, the s is the unknown scale equivalent to Z.
As we know **K**, we can obtain the normalized 2D point $\bar{\mathbf{x}}_j^i = [\bar{x}_j^i \quad \bar{y}_j^i \quad 1]^\intercal$.

$$s\mathbf{K}^{-1}\mathbf{x}_j^i = \tilde{\mathbf{X}}_j^i, \tag{11}$$

$$s\bar{\mathbf{x}}_j^i = \tilde{\mathbf{X}}_j^i, \tag{12}$$

By plugging (12) into (8), the scale s can be computed:

$$s = -\frac{d}{a\bar{x}_j^i + b\bar{y}_j^i + c} \tag{13}$$

As we know s and $\bar{\mathbf{x}}_j^i$, the 3D point on the calibration plane represented in the camera frame $\tilde{\mathbf{X}}$ is obtained. We repeat this process and obtain all $\tilde{\mathbf{X}}_j^i$ on the calibration planes. Finally, we calculate the laser plane equation with all $\tilde{\mathbf{X}}_j^i$ using least squares techniques.

3. SUB-PIXEL LINE DETECTION

In this section, we introduce three sub-pixel line detection methods: the parabola fitting, the weighted average, and the normalized weighted average (proposed method). We compared these three methods, and the results are shown in section 4.

3.1 Parabola Fitting

One of the popular methods for estimating the lines with sub-pixel accuracy is to fit a parabola to the data, and the position of the local maximum of the parabola is the line center. The parabola equation is

$$f(x) = ax^2 + bx + c\,, \tag{14}$$

and if at least three points are given, the unknown parameters of the equation (14) can be solved. The derivative of the equation (14) is

$$f'(x) = 2ax + b\,. \tag{15}$$

As the derivative is zero at the extrema, the local maximum can be obtained where $f'(x) = 0$:

$$x = -\frac{b}{2a}. \tag{16}$$

3.2 Weighted Average

The second method for estimating the line center is to compute the weighted average (center of mass) of the data.

$$x_{subpix} = \frac{\sum_{t=-n}^{n} w_{x+t}\,(x+t)}{\sum_{t=-n}^{n} w_{x+t}}, \tag{17}$$

where w is the image intensity, and n is the mask size to consider. As this approach is much faster and easier to implement than the parabola fitting method when the number of points is not small (e.g. >3), it is widely used in sub-pixel location estimation.

3.3 Normalized Weighted Average

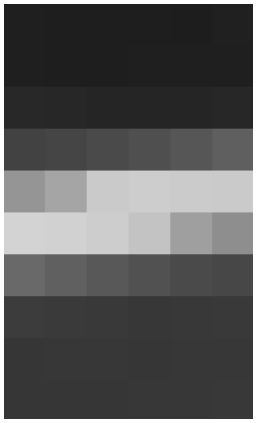

	0	1	2	3	4	5
0	31	30	30	30	29	32
1	31	30	30	31	31	31
2	40	39	37	37	37	39
3	66	69	74	79	86	95
4	149	165	202	**205**	**203**	**202**
5	**211**	**209**	**205**	195	159	142
6	105	96	88	81	74	71
7	60	58	57	55	56	57
8	54	55	55	54	55	55
9	54	54	54	55	55	56

(a) (b)

Figure 3. (a) test image, (b) corresponding intensity of the left image

Although the weighted average method is convenient to use, the centoid may not be correctly computed especially when the number of the data is small. In order to overcome this problem, we first normalize the data and compute the centroid.
Let $\mathbf{w} = [w_{x-n}, \cdots, w_{x-1}, w_x, w_{x+1}, \cdots, w_{x+n}]$ be the intensity of the neighbor of the center pixel x. The normalized weighted average is:

$$\begin{aligned} x_{subpix} &= \frac{\sum_{t=-n}^{n} \big(w_{x+t} - \min(\mathbf{w})\big)(x+t) \big/ \big(\max(\mathbf{w}) - \min(\mathbf{w})\big)}{\sum_{t=-n}^{n} \big(w_{x+t} - \min(\mathbf{w})\big/\big(\max(\mathbf{w}) - \min(\mathbf{w})\big)\big)}, \\ &= \frac{\sum_{t=-n}^{n} \big(w_{x+t} - \min(\mathbf{w})\big)(x+t)}{\sum_{t=-n}^{n} \big(w_{x+t} - \min(\mathbf{w})\big)}. \end{aligned} \tag{18}$$

4. EXPERIMENTAL RESULTS

4.1 Sub-pixeling Results

Figure 3 (a), (b) is the test image and the corresponding intensity at each pixel, respectively. We applied three methods introduced in section 3.

Figure 4 (a), (b) and (c) shows the sub-pixel line estimation results with the parabola fitting, weighted average, and normalized weighted average (proposed method), respectively. NP indicates the nearest pixel that is the position without sub-pixeling. The number of points to be used in the estimation was 3, 5, 7 and 9 at each method. Ideally, the estimated sub-pixel position should be changed smoothly, as the oblique plane was measured.

In figure 4 (a), the points were fitted to the parabola, and the local maximum was computed. When only three points were used (PF3), the estimated sub-pixel position varied smoothly. However, when the number of points was increased, the result was worse (PF5, PF7, PF9). The center position changes suddenly between 2 and 3 in the horizontal axis. This is because the data do not fit

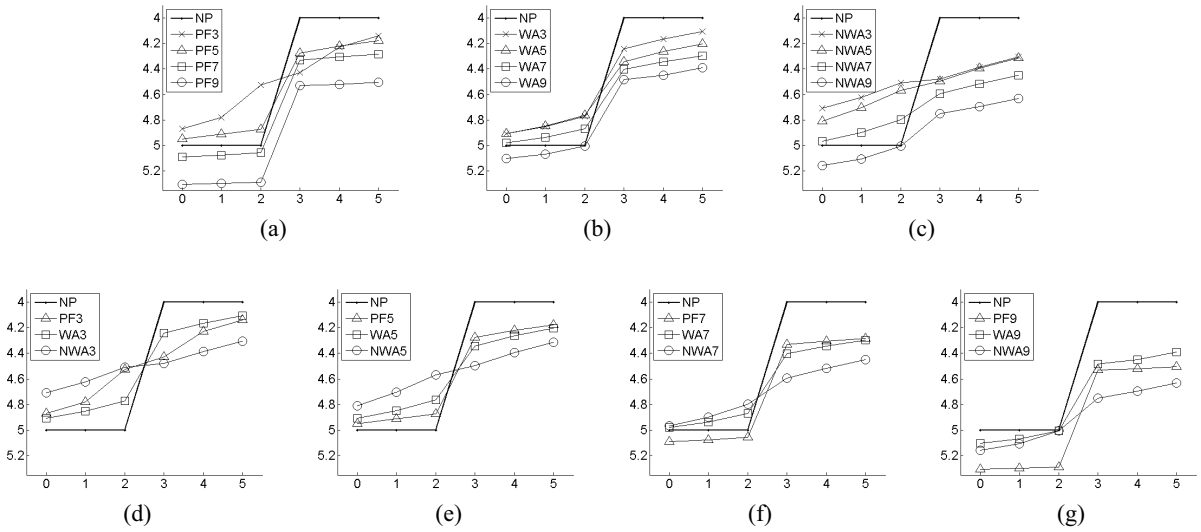

Figure 4. The sub-pixel line estimation results with (a) the parabola fitting, (b) weighted average, and (c) normalized weighted average.

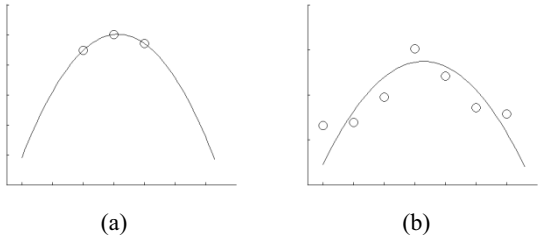

Figure 5. parabola fitting with (a) 3 points, and (b) 7 points.

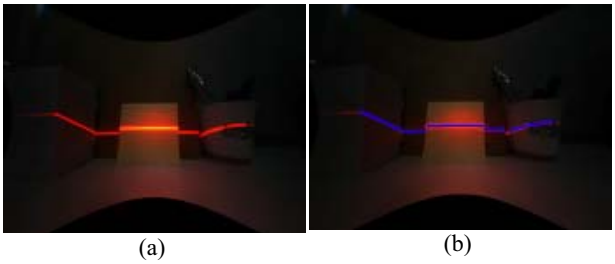

Figure 6. (a) rectified image plane, (b) detected line laser

the parabola.

Figure 5 (a) and (b) show the parabola fitting example when the number of points was 3 and 7, respectively. It is clearly seen that the points do not fit the parabola, so it is not a good idea to use parabola fitting when there is more than five points.

In figure 4 (b), the sub-pixel position was computed by weighted average (i.e., center of mass). Although this method is very popular for sub-pixel location estimation, the results were disappointing regardless of the number of points (see the position between 2 and 3 in the horizontal axis).

In figure 4 (c), the proposed method, normalized weighted average (i.e., normalized center of mass) was applied. The graph shows that the results were desirable from 3 points (NWA3) to 7 points (NWA7). When there are too many points (e.g., 9 points (NWA9)), the results can be bad because the background data (i.e., no line points) affect the estimation. Although the line is slightly spread, this method is still more powerful than others. Its computation time is faster than the parabola least-squares fitting, so it can also be used in real-time applications.

In figure 4 (d) to (g), the results were compared with one another when the same number of points was used. We can see that the normalized weighted average method (NWA3~NWA7) is well suited to the sub-pixel estimation.

4.2 Calibration Results

The lens focal length used in this experiment was 2.1mm and the FOV of the line laser was 120. The distance between the laser plane and the camera was about 40mm. Figure 6 (a) shows the rectified image after undistorting the image with the method in section 3.1, and (b) the detected line laser. The average error was about 0.35mm at 25cm (the distance between the structured light system and the plane).

5. DISCUSSION

In this paper, we proposed a sub-pixel line detection method and a calibration method for wide-angle structured light system. The superiority of the proposed method was verified with several experiments.

REFERENCES

[1] Frederic Devernay, Olivier Faugeras, "Straight lines have to be straight," *Machine Vision and Application*, vol. 13, no. 1 , pp. 14-24, 2001.

[2] Z. Zhang, "A flexible new technique for camera calibration," *IEEE Trans. on Pattern Analysis and Machine Intelligence*, vol. 22, no. 11, pp. 1330-1334, 2000.